

Error Estimation for Reduced-Order Models of Dynamical Systems*

Chris Homescu[†]
Linda R. Petzold[‡]
Radu Serban[§]

Abstract. The use of reduced-order models to describe a dynamical system is pervasive in science and engineering. Often these models are used without an estimate of their error or range of validity. In this paper we consider dynamical systems and reduced models built using proper orthogonal decomposition. We show how to compute estimates and bounds for these errors by a combination of small sample statistical condition estimation and error estimation using the adjoint method. Most important, the proposed approach allows the assessment of *regions of validity* for reduced models, i.e., ranges of perturbations in the original system over which the reduced model is still appropriate. Numerical examples validate our approach: the error norm estimates approximate well the forward error, while the derived bounds are within an order of magnitude.

Key words. model reduction, proper orthogonal decomposition, small sample statistical condition estimation, adjoint method

AMS subject classifications. 65L10, 65L99

DOI. 10.1137/070684392

1. Introduction. Model reduction of dynamical systems described by differential equations is ubiquitous in science and engineering [2]. Reduced-order models (ROMs) are used for efficient simulation [17, 32] and control [18, 28]. Moreover, the process of creating low-order models forces the researcher to isolate and quantify the dominant physical mechanisms, revealing effective design decisions that would not have been identified through numerical simulation, experiments, or “black box” optimization methods [31].

The proper orthogonal decomposition (POD) method has been used extensively in a variety of fields including fluid dynamics [23], identification of coherent structures [12, 21], and control [27] and inverse problems [19]. The method has been em-

*Published electronically May 1, 2007. This paper originally appeared in *SIAM Journal on Numerical Analysis*, Volume 43, Number 3, 2005, pages 1693–1714. This work was supported by grants DOE DE-FG03-00ER25430, NSF/NCSA ACI-9619019, and NSF/ITR ACI-0086061.

<http://www.siam.org/journals/sirev/49-2/68439.html>

[†]Department of Computer Science, University of California, Santa Barbara, CA 93106. Current address: Wachovia Securities, Charlotte, NC 28202 (cristian.homescu@wachovia.com).

[‡]Department of Computer Science, University of California, Santa Barbara, CA 93106 (petzold@engineering.ucsb.edu).

[§]Center for Applied Scientific Computing, Lawrence Livermore National Laboratory, Livermore, CA 94551 (radu@llnl.gov). The work of this author was performed under the auspices of the U.S. Department of Energy by the University of California, Lawrence Livermore National Laboratory, under contract W-7405-Eng-48.

ployed for industrial applications such as supersonic jet modeling [5], turbine flows [6], thermal processing of foods [3], and study of the dynamic wind pressures acting on buildings [16], to name only a few.

Depending on the field of research, POD is also known as principal component analysis (statistics [14]), Karhunen–Loève decomposition (signal analysis and pattern recognition [9]), and the method of empirical orthogonal functions (EOFs) in geophysical fluid dynamics [7, 24] and meteorology [1, 8, 29]. Techniques based on principal component analysis (PCA) are the main dimension-reduction methods in analysis of multivariate data, addressing the need to compress or decompose data for eliminating the redundancy of high throughput measurements such as spatial, spectra, or image data. PCA involves a mathematical procedure that transforms a number of (possibly) correlated variables into a (smaller) number of uncorrelated variables called principal components. The PCA components account for as much of the variability in the data as possible. The EOFs form a set of basis functions which specify a transformation on a set of empirical signals. The result is a set of signals that, phenomenologically speaking, are statistically independent, i.e., have maximum variance. Thus, information is evenly distributed among the signals, as well as the equally measurable values of each signal, resulting in maximum information entropy and robustness to noise.

All the above reduction methods attempt to maximize the expectation of the energy in a basis set. It was shown that such an optimal basis is given by the eigenfunctions of the integral equation whose kernel is the averaged autocorrelation function. In practice, the covariance matrix is constructed based on measurements of the state, and the existing model projected onto those eigenvectors which correspond to the largest eigenvalues. Assessing the optimality of these reduction methods (POD, PCA, and EOF) is a *norm-dependent* statement. For example, it was shown in [12] that for a given number of modes, POD is the most efficient choice among all linear decompositions in the sense that it retains, on average, the greatest possible kinetic energy.

For analyses that require numerous and repeated solutions of the dynamical system (such as dynamic optimization, control, etc.), ROMs are particularly appealing for efficiency considerations. The reduction in dimension—and thus cost of simulation—can be dramatic, and yet the resulting ROM can very accurately reproduce the solution of the full-scale model. For example, Ma and Karniadakis [23] report on a POD-based ROM for the flow past a circular cylinder which, with as few as 40 modes, can accurately reproduce limit cycles and bifurcations obtained with a high-resolution direct numerical simulation using hundreds of thousands of degrees of freedom.

However, an important property of nonlinear ROMs is that they are necessarily based on a nominal set of parameters but are commonly used to obtain the system solution at a different set of parameters. As such, as soon as one contemplates the use of a reduced model, questions concerning the quality of the approximation (particularly under perturbations of the nominal parameters used in building the ROM) become paramount. To judge the quality of the reduced model, it is important to estimate its error.

An algorithm for estimating the error of a class of reduction methods based on projection techniques was presented in [33]. In this approach, the original problem is linearized around the initial time. The resulting first-order error estimates are valid for only a small number of time steps (during which the Jacobian matrix can be considered constant). First-order estimates of POD errors were used in [20] to extend the concept of domain decomposition as a dynamic a posteriori verification and, if necessary, correction of the approximate solution. Error estimates for reduced models, more precisely the error for certain functionals of the solution, were obtained

in [25]. The authors employed the dual-weighted-residual method, which makes use of the solution of an adjoint system.

In the context of fluid dynamics, bounds for the errors resulting from POD model reduction of two-dimensional Navier–Stokes equations were computed in [19]. In that work, the approximation error was decomposed into a contribution that arises due to the POD spatial approximation (measured in terms of the spectral properties specifying the POD basis) and the approximation error due to the backward Euler scheme for time integration. The resulting estimates made use of certain inequalities that, although valid for the nonlinear evolution problem considered, may not be satisfied for other examples. For models that contain discontinuities, for example, if the solution involves shocks, it was found in [22] that the POD reduced model was able to represent a shock in a given location only if one of the snapshots used to build the model had a discontinuity in the same location. This may require an unacceptably large number of snapshots to achieve sufficient accuracy of the approximate solution. To overcome this limitation a domain decomposition technique was introduced, using a reduced-order model over the majority of the computational domain while solving the full equations in a small region. Given an approximate solution (with unknown accuracy) generated with a set of POD basis functions, the error is estimated by augmenting the POD basis with top hat basis functions and computing the first-order change in the solution due to the additional basis functions. By comparing against the results from a solution of known accuracy, such as one of the snapshots used to generate the POD basis, the need for domain decomposition and its spatial extent can be determined.

Bounds of POD errors, but not estimates, were considered in [26], as well as effects (on the reduced-order model) of small perturbations in the ensemble of data from which the POD reduced-order model was constructed.

In the present work we take the analysis of reduced models one step further by analyzing the influence of perturbations to the original system on the quality of the approximation given by the reduced model. This question is of particular interest in applications (such as control and inverse problems) in which reduced models are used not just to approximate the solution of the original system that provided the data used in constructing the reduced model, but rather to approximate the solution of systems perturbed from the original one. To the best of our knowledge, there are no published results that address the estimation of the model reduction error of such perturbed systems.

We base our approach on a combination of the small sample statistical condition estimation (SCE) method [15] and error estimation using the adjoint method. Using this framework, we define *regions of validity* of the reduced models, that is, ranges of perturbations in the original system over which the reduced model is still appropriate. We consider perturbations in both the initial conditions and in parameters describing the dynamical system itself. The proposed approach is particularly attractive because the resulting error bounds do not rely on the solution of the perturbed system. In this sense, we provide an a priori assessment of the validity of the model-reduction approximation. We note that our approach is based on linearization. For large enough perturbations, knowledge of the solution of the perturbed system would be required.

Unlike the method presented in [33], our estimates and bounds are valid over the entire time interval considered, not in a neighborhood of the initial time. Moreover, we obtain estimates for the continuous error, as opposed to its discrete approximation. Although we study only a particular projection-based model reduction technique (POD) among those considered in [33], the methodology developed here for POD can

be easily extended to other types of projection. Compared to the approach taken in [19], our method is applicable to a larger class of problems, our main requirement being that the norm of the POD-based error is small enough for the linearized error equation to be a good enough approximation. Furthermore, our estimates are independent of the time integration method. We note also that our use of adjoint models for error estimation is similar to that employed in [25]. However, as will be seen below, the use of the SCE method enables the derivation of error “condition numbers” and allows effective treatment of the region of validity problem.

In the context of integration of ordinary differential equations (ODE), the SCE method combined with the adjoint approach has been used in [4] for estimation and control of the global integration error.

The remainder of this paper is organized as follows. In sections 2 and 3 we briefly describe the use of POD for model reduction and, respectively, the SCE method for norm estimation. In section 3.1 we motivate our proposed approach of using SCE, combined with error estimation using the adjoint method, to estimate the errors due to the use of a reduced-order model. In section 4 we analyze errors arising purely from the model reduction itself: the total approximation error and the subspace integration error. In section 5 we analyze regions of validity of POD reduced models. In section 6 we present numerical results for two example problems. The first one is obtained from the semidiscretization of time-dependent partial differential equation (PDE), namely, advection-diffusion, while the second example models a pollution chemical reaction mechanism. Finally, section 7 summarizes our results and describes our plans for future research.

2. POD-Based Reduced Models. POD provides a method for finding the best approximating affine subspace to a given set of data. When using POD for model reduction of dynamical systems, the data are time snapshots of the solution obtained via numerical simulations or from experiments. Consider the ODE system

$$(2.1) \quad \frac{dy}{dt} = f(y, t), \quad y(t_0) = y_0,$$

for $t \in [t_0, t_f]$, with $y, y_0 \in R^n$ and $f : R^n \times R \rightarrow R^n$. Consider next the solutions of (2.1) at m time points, collected in the $n \times m$ matrix $\mathcal{Y} = [y(t_1) - \bar{y}, y(t_2) - \bar{y}, \dots, y(t_m) - \bar{y}]$, where \bar{y} is the mean of these observations. POD seeks a subspace $S \in R^n$ and the corresponding projection matrix P_S so that the total square distance

$$\|\mathcal{Y} - P\mathcal{Y}\|^2 = \sum_{i=1}^m \|(y(t_i) - \bar{y}) - P(y(t_i) - \bar{y})\|^2$$

is minimized. Let $\lambda_1 \geq \lambda_2 \geq \dots \geq \lambda_m \geq 0$ be the ordered eigenvalues of the *correlation matrix* $R = \mathcal{Y}\mathcal{Y}^T$. Then the minimum value of $\|\mathcal{Y} - P\mathcal{Y}\|^2$ over all k -dimensional subspaces S , with $k \leq n$, is given by $\sum_{j=k+1}^n \lambda_j$. Moreover, the minimizing S is the invariant subspace corresponding to the eigenvalues $\lambda_1, \dots, \lambda_k$. Using the singular value decomposition (SVD) [10] of the observation matrix, $U^T \mathcal{Y} V = \Sigma$, the projection matrix corresponding to the optimal POD subspace S is obtained as

$$(2.2) \quad P = \rho \rho^T \in R^{n \times n},$$

where ρ is the matrix of projection onto S , the subspace spanned by the reduced basis obtained from the SVD. The matrix $\rho \in R^{n \times k}$ consists of the columns V_i ($i = 1, \dots, k$), the singular vectors corresponding to the k largest singular values.

Without loss of generality, for the sake of simplicity in presentation we assume in what follows that $\bar{y} = 0$.

In a coordinate system embedded in S , the projection of a point $y \in R^n$ onto S is represented by $z = \rho^T y \in R^k$, while in the full space the same projection is expressed as $\rho z = P y \in R^n$.

A POD-based reduced model that approximates the original problem (2.1) can then be constructed [26] by projecting onto S the vector field $f(y, t)$ at each point $y \in S$. Therefore

$$(2.3) \quad \frac{dz}{dt} = \rho^T f(\rho z, t), \quad z(t_0) = \rho^T y_0.$$

In full space, the approximate solution \tilde{y} is the solution of the ODE initial-value problem (IVP)

$$(2.4) \quad \frac{d\tilde{y}}{dt} = P f(\tilde{y}, t), \quad \tilde{y}(t_0) = P y_0.$$

3. Small Sample Statistical Method for Condition Estimation. The SCE method, originally proposed in [15], offers an efficient means for condition estimation for general matrix functions, at the cost of allowing moderate relative errors in the estimate. The basic idea is described below (for complete details, see [11, 15]).

For any vector $x \in R^n$, if u is selected uniformly and randomly from the unit sphere S_{n-1} , the expected value of $u^T x$ is proportional to the norm of x :

$$E(|u^T x|) = W_n \|x\|.$$

The *Wallis factor* W_n is defined as

$$W_1 = 1, \quad W_n = \begin{cases} \frac{1 \cdot 3 \cdots (n-2)}{2 \cdot 4 \cdots (n-1)}, & n \text{ odd,} \\ \frac{2 \cdot 2 \cdot 4 \cdots (n-2)}{\pi \cdot 1 \cdot 3 \cdots (n-1)}, & n \text{ even,} \end{cases}$$

and can be approximated with $W_n \approx \sqrt{2/(\pi(n-1/2))}$. Therefore $\xi = |u^T x|/W_n$ is an estimate for the norm $\|x\|$. This estimate is first order in the sense that the probability of a relative error in the estimate is inversely proportional to the size of the error. That is, for $\gamma > 1$,

$$\Pr \left(\frac{\|x\|}{\gamma} \leq \xi \leq \gamma \|x\| \right) \geq 1 - \frac{2}{\pi\gamma} + O(\gamma^{-2}).$$

Additional function evaluations can improve the estimation procedure. Suppose that we obtain estimates $\xi_1, \xi_2, \dots, \xi_q$ corresponding to orthogonal vectors u_1, u_2, \dots, u_q selected uniformly and randomly from the unit sphere S_{n-1} . The expected value of the norm of the projection of x onto the span \mathcal{U} generated by u_1, u_2, \dots, u_q is

$$E \left(\sqrt{|u_1^T x|^2 + |u_2^T x|^2 + \cdots + |u_q^T x|^2} \right) = \frac{W_n}{W_q} \|x\|.$$

The analysis in [15] shows that the estimate $\nu(q) = (W_q/W_n) \sqrt{|u_1^T x|^2 + \cdots + |u_q^T x|^2}$ is q th order accurate; i.e., a relative error of size γ in the estimate occurs with prob-

ability proportional to γ^{-q} . For example,

$$\begin{aligned}\Pr\left(\frac{\|x\|}{\gamma} \leq \nu(2) \leq \gamma\|x\|\right) &\approx 1 - \frac{\pi}{4\gamma^2}, \\ \Pr\left(\frac{\|x\|}{\gamma} \leq \nu(3) \leq \gamma\|x\|\right) &\approx 1 - \frac{32}{3\pi^2\gamma^3}, \\ \Pr\left(\frac{\|x\|}{\gamma} \leq \nu(4) \leq \gamma\|x\|\right) &\approx 1 - \frac{81\pi^2}{512\gamma^4}.\end{aligned}$$

3.1. SCE for Estimation of Approximation Errors in Model Reduction. All error estimates derived in this paper begin with the linearizations of one of the ODEs (2.1), (2.3), or (2.4), or perturbations of these. Thus the error estimates are based on solutions of linear error equations. To estimate the norm $\|e(t_f)\|$ of an error vector $e(t) \in R^n$ at $t = t_f$, we need to evaluate quantities $u_j^T e(t_f)$ for some random vector u_j selected uniformly from the unit sphere S_{n-1} . The norm estimate is then

$$(3.1) \quad \|e(t_f)\| \approx \frac{W_q}{W_n} \sqrt{\sum_{j=1}^q |u_j^T e(t_f)|^2}.$$

The scalar products $u_j^T e(t_f)$ can be computed efficiently using an adjoint model (to the corresponding linear error equation) with final conditions at t_f based on the vector u_j . However, this approach naturally raises the question: “*What is the advantage of using (typically more than one) solution(s) of the adjoint system to estimate the norm of a quantity that can be otherwise obtained with only one forward ODE solution (of the error equation)?*” Our method is motivated by the fact that we are interested not only in estimating the error for one given ODE system, but rather in estimating (as efficiently as possible) the behavior of such errors for families of related ODE systems, based on different values of problem parameters. In section 5 we study the concept of *regions of validity of reduced models*, i.e., the range of perturbations in the original ODE (2.1) over which the reduced model (2.3) is still appropriate. An approach based on forward error equations involves solving repeatedly such error equations (for each value of interest of the perturbation). On the other hand, an approach combining SCE estimates and adjoint models (as described in our paper) can be used to define what we term “condition numbers” for these error equations. While these condition numbers can provide only approximate upper bounds for the norms of the errors under investigation, they have the undeniable advantage of allowing a priori estimates of the errors induced by perturbations, i.e., before having to solve such a perturbed system (or even a reduced perturbed system).

4. Estimation of the Approximation Error. We begin by estimating the difference between the solution of the POD-reduced model (2.4) and the solution of the original equation (2.1). The total approximation error $e = \tilde{y} - y$ can be split [26] into the subspace approximation error $e_{\perp} = \rho^T y - y$ and the error introduced by the integration in the subspace S , $e_S = \tilde{y} - \rho^T y$:

$$(4.1) \quad e = \tilde{y} - y = (\tilde{y} - \rho^T y) + (\rho^T y - y) = e_S + e_{\perp}.$$

The error component e_{\perp} is orthogonal to S , while the component e_S is parallel to S (see Figure 1). Algebraically, this is expressed as $Pe_{\perp}(t) = 0$ and $Pe_S(t) = e_S(t)$.

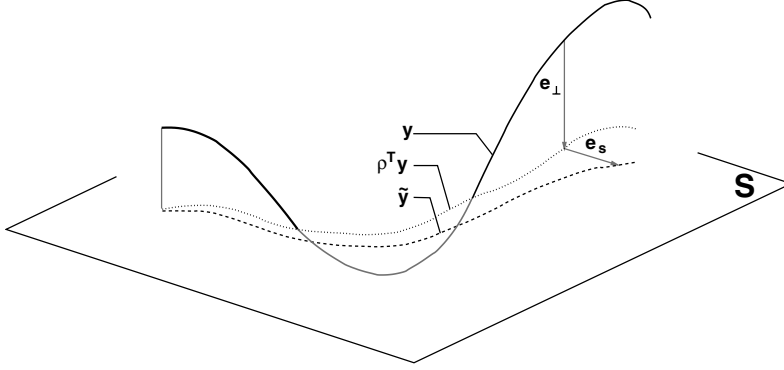


Fig. 1 Solution and error components for POD-reduced models. y is the solution of the original ODE, $z = \rho^T y$ is its projection on the subspace S , and \tilde{y} is the solution of the reduced model. The error component $e_{\perp} \in S^{\perp}$, while the subspace integration error component $e_S \in S$.

4.1. Total Approximation Error. Subtracting (2.1) from (2.4) yields an equation for the total error e ,

$$\begin{aligned} \frac{de}{dt} &= Pf(\tilde{y}, t) - f(y, t) = Pf(\tilde{y}, t) - f(\tilde{y}, t) + f(\tilde{y}, t) - f(y, t) \\ &= (P - I)f(\tilde{y}, t) - \mathbf{J}(\tilde{y}, t)(y - \tilde{y}) + O(\|e\|), \end{aligned}$$

where \mathbf{J} is the Jacobian of the function f , i.e., $\mathbf{J} = \partial f / \partial y$, and we define $Q = I - P$. Thus, to a first-order approximation, the error function satisfies

$$(4.2) \quad \frac{de}{dt} = \mathbf{J}(\tilde{y}, t)e(t) - Qf(\tilde{y}, t), \quad e(t_0) = -Qy_0.$$

Let the matrix function $\Phi(t) \in R^{n \times n}$ satisfy

$$\frac{d\Phi}{dt} = \mathbf{J}(\tilde{y}, t)\Phi, \quad \Phi(t_0) = I_n.$$

Then

$$e(t_f) = - \int_{t_0}^{t_f} \Phi(t_f)\Phi^{-1}(\tau)Qf(\tilde{y}(\tau), \tau) d\tau - \Phi(t_f)Qy_0.$$

For a random vector u uniformly selected from the unit sphere S_{n-1} , we have

$$u^T e(t_f) = - \int_{t_0}^{t_f} u^T \Phi(t_f)\Phi^{-1}(\tau)Qf(\tilde{y}(\tau), \tau) d\tau - u^T \Phi(t_f)Qy_0.$$

It is straightforward to verify that the solution $\lambda \in R^n$ of the adjoint system,

$$(4.3) \quad \frac{d\lambda}{dt} = -\mathbf{J}^T(\tilde{y}, t)\lambda, \quad \lambda(t_f) = u,$$

satisfies $\lambda^T(s) = u^T \Phi(t_f)\Phi^{-1}(s)$ and $\lambda^T(t_0) = z^T \Phi(t_f)$. Therefore the quantity $u^T e(t_f)$ is simply

$$(4.4) \quad u^T e(t_f) = - \int_{t_0}^{t_f} \lambda^T(\tau)Qf(\tilde{y}(\tau), \tau) d\tau - \lambda^T(t_0)Qy_0.$$

The SCE estimate for the norm of $e(t_f)$ is obtained by combining (3.1) and (4.4):

$$(4.5) \quad \|e(t_f)\| \approx \frac{W_q}{W_n} \sqrt{\sum_{j=1}^q \left| \int_{t_0}^{t_f} \lambda^T(\tau) Q f(\tilde{y}(\tau), \tau) d\tau + \lambda^T(t_0)^T Q y_0 \right|^2}.$$

The value of the integral is $\xi(t_0)$, where ξ satisfies the quadrature equation

$$(4.6) \quad \frac{d\xi}{dt} = -\lambda^T(t) Q f(\tilde{y}(t), t), \quad \xi(t_f) = 0.$$

Algorithm 1 summarizes our approach.

ALGORITHM 1. Estimate for the total approximation error.

Provide the matrix of measurement data \mathcal{Y}

Set the POD dimension k

Construct POD projection matrices ρ and P

Select uniformly and randomly q orthogonal vectors u_i from the unit sphere S_{n-1}

Solve (2.3) for z and compute $\tilde{y}(t) = \rho z(t)$

Initialize $s = 0$

for $i = 1$ to q **do**

 Set $\lambda(t_f) = u_i$ and $\xi(t_f) = 0$

 Solve (4.3)+(4.6) for λ and ξ

 Update $s \leftarrow s + [\psi(t_0) + \lambda^T(t_0)^T Q y_0]^2$

end for

Compute Wallis factors W_q and W_n

Compute the SCE norm estimate $\|e\| = (W_q/W_n) \cdot \sqrt{s}$

It may seem more efficient to compute the SCE norm estimate using a POD-reduced adjoint system to evaluate λ in (4.5). Although the same projection can be used to model-reduce the adjoint system, this approach still requires knowledge of the mean of the adjoint solution, which is unavailable without a solution of the adjoint system (4.3). In other words, the approximation subspace is parallel to S but not identical to it. This issue can be circumvented if we are not considering error components outside the subspace S . This estimate is presented next. Its main advantage is given by the fact that the differential equations are solved in a space of dimension $k \ll n$, where n is the dimension of the solution for the original problem.

4.2. Subspace Integration Error. Starting with its definition, $e_S = \tilde{y} - \rho^T y$, the subspace integration error is readily found to obey, in a first-order approximation, the following ODE:

$$\begin{aligned} \frac{de_S}{dt} &= \frac{d\tilde{y}}{dt} - P \frac{dy}{dt} = P \left(f(\tilde{y}, t) - f(y, t) \right) \\ &\approx P \mathbf{J}(\tilde{y}, t) e(t) = P \mathbf{J}(\tilde{y}, t) (e_S + e_\perp). \end{aligned}$$

The starting point $\tilde{y}(t_0)$ is the projection $\rho^T y(t_0)$ of $y(t_0)$ onto S , yielding the initial condition $e_S(t_0) = 0$. Thus, the subspace integration error is governed by an ODE with the subspace approximation error $e_\perp(t)$ as forcing term,

$$(4.7) \quad \frac{de_S}{dt} = P \mathbf{J}(\tilde{y}, t) e_S + P \mathbf{J}(\tilde{y}, t) e_\perp, \quad e_S(t-0) = 0.$$

We note that the linearization in (4.7) is directly related (through the projection

matrix P) to the linearization of the full model, $f(\tilde{y}, t) - f(y, t) \approx \mathbf{J}(\tilde{y}, t)(\tilde{y} - y)$. Since we assume that we operate in a region where the full model linearization is valid, this implies that the linearization in (4.7) is valid for the region considered.

If h are the S -coordinates of e_S , i.e., $h = \rho^T e_S \in R^k$, we have $e_S = \rho h$ and therefore

$$(4.8) \quad \frac{dh}{dt} = \rho^T \mathbf{J}(\tilde{y}, t) \rho h + \rho^T \mathbf{J}(\tilde{y}, t) e_{\perp}, \quad h(t_0) = 0,$$

where we have used that $\rho^T \rho = I_k$. Now let $\psi \in R^{k \times k}$ be the fundamental matrix of (4.8); i.e.,

$$\frac{d\psi}{dt} = \rho^T \mathbf{J}(\tilde{y}, t) \rho \psi, \quad \psi(t_0) = I_k.$$

Then, for a random vector v uniformly selected from the unit sphere S_{k-1} , we have

$$v^T h(t_f) = \int_{t_0}^{t_f} v^T \psi(t_f) \psi^{-1}(\tau) \rho^T \mathbf{J}(\tilde{y}(\tau), \tau) e_{\perp}(\tau) d\tau.$$

The solution μ of the adjoint system

$$(4.9) \quad \frac{d\mu}{dt} = -\rho^T \mathbf{J}^T(\tilde{y}, t) \rho \mu, \quad \mu(t_f) = v,$$

satisfies $\mu^T(\tau) = v^T \psi(t_f) \psi^{-1}(\tau)$ for all $\tau \in [t_0, t_f]$, and therefore

$$v^T h(t_f) = \int_{t_0}^{t_f} \mu^T(\tau) \rho^T \mathbf{J}(\tilde{y}(\tau), \tau) e_{\perp}(\tau) d\tau,$$

yielding the following SCE estimate for the norm of the subspace integration error:

$$(4.10) \quad \|e_S(t_f)\| = \|h(t_f)\| \approx \frac{W_q}{W_n} \sqrt{\sum_{j=1}^q \left| \int_{t_0}^{t_f} \mu_j^T(\tau) \rho^T \mathbf{J}(\tilde{y}(\tau), \tau) e_{\perp}(\tau) d\tau \right|^2},$$

where μ_j is the solution of (4.9) with final condition $\mu(t_f) = v_j$.

Bounds for the subspace integration error can be obtained as follows. We have

$$\begin{aligned} \left| \int_{t_0}^{t_f} \mu^T(\tau) \rho^T \mathbf{J}(\tilde{y}(\tau), \tau) e_{\perp}(\tau) d\tau \right| &\leq \int_{t_0}^{t_f} \left| \mu^T(\tau) \rho^T \mathbf{J}(\tilde{y}(\tau), \tau) e_{\perp}(\tau) \right| d\tau \\ &\leq \|\mathbf{J}^T \rho \mu\|_{L_1} \cdot \|e_{\perp}\|_{L_{\infty}}, \end{aligned}$$

where the last inequality is Hölder's inequality, $\|f^T g\|_{L_1} \leq \|f\|_{L_p} \cdot \|g\|_{L_q}$, $1/p + 1/q = 1$, for $p = 1$ and $q = \infty$, applied to vector-valued functions $f, g : [t_0, t_f] \rightarrow R^n$ for which the L_p norm is defined as

$$\|f\|_{L_p} = \left(\int_{t_0}^{t_f} \|f(\tau)\|_p^p d\tau \right)^{1/p}, \quad \text{where } \|f(\tau)\|_p = \left(\sum_{i=1}^n |f_i(\tau)|^p \right)^{1/p}.$$

Therefore

$$(4.11) \quad \|e_S(t_f)\| \leq \kappa(e_S) \cdot \|e_{\perp}\|_{L_{\infty}},$$

where

$$\kappa(e_S) = \frac{W_q}{W_n} \sqrt{\sum_{j=1}^q \|\mathbf{J}^T \rho \mu_j\|_{L_1}^2} = \sqrt{\sum_{j=1}^q \left(\int_{t_0}^{t_f} \left| \mathbf{J}^T(\tilde{y}(\tau), \tau) \rho \mu_j(\tau) \right| d\tau \right)^2}.$$

The quantity $\kappa(e_S)$ can be seen as a ‘‘condition number’’ for the subspace integration error.

The expressions derived above require knowledge of the projection error e_\perp at all times in $[t_0, t_f]$. While the projection error may not be readily available, its norm can be easily related to the error associated with the choice of the POD subspace. For this, a more convenient formulation of the POD approximation is to find a subspace $S \subset R^n$ which minimizes the total square distance defined as

$$(4.12) \quad d^2 = \|y - Py\|_{L_2}^2 = \int_{t_0}^{t_f} \|y(\tau) - Py(\tau)\|_2^2 d\tau.$$

The solution to this problem requires the construction of the correlation matrix $R = \int_{t_0}^{t_f} y(\tau)y(\tau)^T d\tau$. If $\lambda_1 \geq \dots \geq \lambda_m \geq 0$ are the ordered eigenvalues of the symmetric positive semidefinite matrix R , then the minimum value of d^2 over all k -dimensional affine subspaces S passing through \bar{y} is given by $\sum_{j=k+1}^n \lambda_j$. The minimizing S is the invariant subspace corresponding to the eigenvalues $\lambda_1, \dots, \lambda_k$, while the projection matrix ρ consists of the unit eigenvectors corresponding to these k largest eigenvalues. We also have that

$$\|e_\perp\|_{L_\infty} \leq \|e_\perp\|_{L_2} \equiv \sqrt{\sum_{j=k+1}^n \lambda_j}.$$

Employing observations as data points for a trapezoidal approximation for the integral (4.12) leads to the same subspace S as the one obtained with the POD definition in section 2, while the corresponding optimal total square distances will be proportional.

5. Regions of Validity for POD-Reduced Models. Once a reduced model is constructed, we wish to apply it to simulate systems that are close in some sense to the system that was used for generating the reduced model. This raises the issue of defining the range of initial conditions and parameters over which the reduced model can be used with acceptable accuracy.

In the following section we denote by a lowercase letter (e.g., y) any solution of the unperturbed system and by a capital letter (e.g., Y) any solution of a perturbed system.

If $Y \in R^n$ is the solution of an ODE obtained by applying a perturbation to (2.1), either in the initial conditions or in the right-hand side, the issue of the errors introduced by this perturbation, in addition to the model reduction error $e(t)$, can be addressed from two different perspectives:

- When the reduced model, with a POD projection matrix based on the solution of the unperturbed ODE, is used to approximate the perturbed solution Y , it is of interest to estimate the error $E_1 = \tilde{Y} - Y$, where \tilde{Y} is the solution of an ODE of the form (2.4), with P based on y .
- Alternatively, we may want estimates for the cumulative error (due to the POD model reduction and the perturbation in the original ODE), $E_2 = \tilde{Y} - y$. Note that calculating $E_2 = \tilde{Y} - y$ is completely equivalent to computing $\tilde{y} - Y$ (by considering y to be a perturbation to Y).

It is important to realize that *useful* estimates should not rely on the solution Y (or \tilde{Y}) of the perturbed system (or its POD reduction). Indeed, such error estimates are desired with the sole objective of deciding whether or not to solve these systems.

In this section we begin by analyzing the errors E_1 and E_2 induced by a perturbation δy_0 in the initial conditions of (2.1) and then by treating the case of perturbations δp in model parameters affecting the right-hand side. For each of these two cases, Figure 2 illustrates the solutions of the unperturbed and perturbed full- and reduced-order models, as well as the corresponding errors e , E_1 , and E_2 .

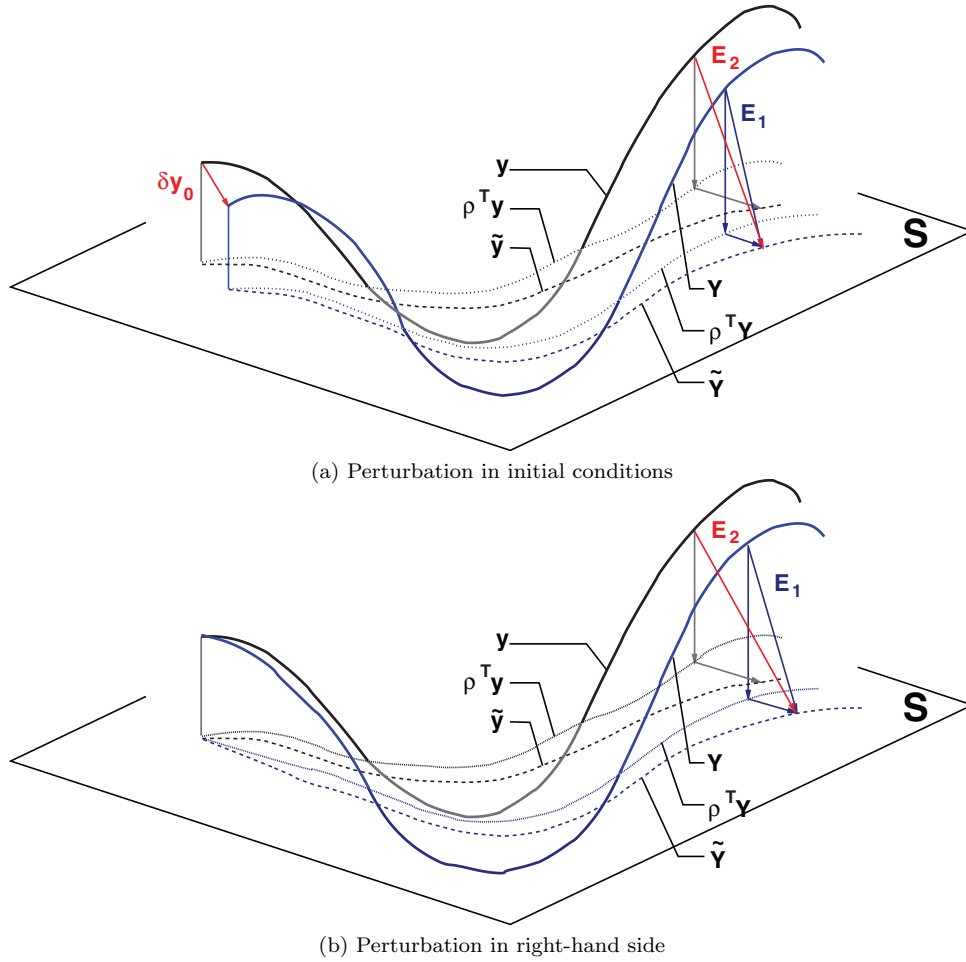


Fig. 2 Error components in model reduction of perturbed systems. The solution of the perturbed system and the solution of the reduced perturbed system are denoted by Y and \tilde{Y} , respectively. The error E_1 represents the error committed in reducing the perturbed model, while E_2 is the cumulative error (perturbation + model reduction).

5.1. Perturbations in Initial Conditions. Here, Y and \tilde{Y} are solutions of the ODEs

$$(5.1) \quad \frac{dY}{dt} = f(Y, t), \quad Y(t_0) = Y_0 = y_0 + \delta y_0,$$

$$(5.2) \quad \frac{d\tilde{Y}}{dt} = Pf(\tilde{Y}, t), \quad \tilde{Y}(t_0) = PY_0 = P(y_0 + \delta y_0),$$

which were obtained by perturbing the initial conditions of (2.1).

5.1.1. Estimation of $E_1 = \tilde{Y} - Y$. An SCE estimate like (4.5) is not useful in the sense described above, as it would be based on the error equation

$$(5.3) \quad \frac{dE_1}{dt} = \mathbf{J}(\tilde{Y}, t)E_1 - Qf(\tilde{Y}, t), \quad E_1(t_0) = -Q(y_0 + \delta y_0 - \bar{y}),$$

which is a linearization around the (unknown) trajectory $\tilde{Y}(t)$.

Instead, let us focus on estimating the norm of $\Delta(t_f) = E_1(t_f) - e(t_f)$, with which the norm $\|E_1(t_f)\|$ could be bounded by

$$(5.4) \quad \left| \|e(t_f)\| - \|\Delta(t_f)\| \right| \leq \|E_1(t_f)\| \leq \|e(t_f)\| + \|\Delta(t_f)\|.$$

Any estimates of $\|\Delta(t_f)\|$ would require solving the POD-reduced perturbed system (5.2). However, as in section 4.2, this problem can be circumvented by splitting the error Δ into two components: Δ_\perp orthogonal to S and Δ_S parallel to S . Using the fact that $Q\tilde{Y} = Q\tilde{y} = 0$, we have

$$\Delta_\perp = Q\Delta = Q(\tilde{Y} - \tilde{y}) - (Y - y) = -Q(Y - y)$$

and

$$\Delta_S = \Delta - \Delta_\perp = (\tilde{Y} - \tilde{y}) - P(Y - y).$$

We evaluate the influence of δy_0 on each component separately. Retaining only the first-order term of a Taylor series for Δ_\perp around $\delta y_0 = 0$ and using the fact that $\Delta_\perp = 0$ for $\delta y_0 = 0$, we get

$$\Delta_\perp = -Q \left. \frac{dY}{d\delta y_0} \right|_{\delta y_0=0} \delta y_0.$$

The sensitivity matrix dY/dy_0 is nothing but the fundamental matrix corresponding to the linearization of (2.1). It is then easy to see that if λ is now the solution of

$$(5.5) \quad \frac{d\lambda}{dt} = -\mathbf{J}^T(y, t)\lambda, \quad \lambda(t_f) = Qu \quad \text{for some } u \in R^n,$$

then $u^T \Delta_\perp(t_f) = -\lambda^T(t_0) \cdot \delta y_0$.

Therefore, an SCE estimate of $\|\Delta_\perp(t_f)\|$ can be based on the solutions of systems (5.5) with vectors u_j uniformly and randomly selected from the unit sphere S_{n-1} . However, taking into account that Δ_\perp is orthogonal to S , a more accurate estimate can be obtained by using vectors from the sphere S_{n-k-1} embedded in S^\perp , instead of selecting vectors $u \in S_{n-1}$ and projecting them onto S^\perp , the orthogonal complement of S . If u' is the representation in R^n of such a vector, then $Qu' = u'$. Thus we have the same adjoint system (5.5), but the probability that the estimate lies within a given factor γ of the true norm $\|\Delta_\perp(t_f)\|$ is now higher (see section 3).

In practice we use the approximation $y \approx \tilde{y}$ in evaluating the Jacobian in (5.5), with \tilde{y} computed from the solution z of the k -dimensional ODE (2.3), and obtain the following SCE estimate:

$$\|\Delta_\perp(t_f)\| \approx \frac{W_q}{W_n} \sqrt{\sum_{j=1}^q |u_j'^T \Delta_\perp(t_f)|^2} = \frac{W_q}{W_n} \sqrt{\sum_{j=1}^q |\lambda^T(t_0) \delta y_0|^2},$$

where λ is the solution of $d\lambda/dt = -\mathbf{J}^T(\tilde{y}, t)\lambda$, $\lambda(t_f) = Qu'_j$. Hölder's inequality (for $p = q = 2$) gives $|\lambda^T(t_0) \delta y_0| \leq \|\lambda(t_0)\|_2 \cdot \|\delta y_0\|_2$, which implies

$$(5.6) \quad \|\Delta_\perp(t_f)\| \leq \kappa_1 \cdot \|\delta y_0\|,$$

where the ‘‘condition number’’ for the orthogonal component of Δ is defined as

$$\kappa_1 = \frac{W_q}{W_n} \sqrt{\sum_{j=1}^q \|\lambda(t_0)\|_2^2}.$$

With the assumption $\mathbf{J}(y, t) \approx \mathbf{J}(\tilde{y}, t)$, the Δ component parallel to S , $\Delta_S = \Delta - \Delta_\perp = (\tilde{Y} - \tilde{y}) - P(Y - y)$, satisfies, up to first order,

$$\frac{d\Delta_S}{dt} = \left(Pf(\tilde{Y}, t) - Pf(\tilde{y}, t) \right) - P(f(Y, t) - f(y, t)) \approx P\mathbf{J}(\tilde{y}, t)\Delta_S.$$

Since at the initial time $\Delta_S(t_0) = 0$, to a first-order approximation $\Delta_S(t) = 0$ for all $t \geq t_0$. In other words, a perturbation to the initial conditions of the original ODE does not introduce additional subspace integration errors. As a consequence, $\Delta(t_f) \approx \Delta_\perp(t_f)$ and, combining (5.4) and (5.6), we have

$$(5.7) \quad \|E_1(t_f)\| \leq \|e(t_f)\| + \kappa_1 \cdot \|\delta y_0\|.$$

Note that when using SCE estimates for the norms involved in the above bounds, the true value of $\|E_1(t_f)\|$ may not be bracketed by these bounds.

5.1.2. Estimation of $E_2 = \tilde{y} - Y$. Subtracting the ODEs satisfied by \tilde{y} and Y , the error E_2 satisfies, to a first-order approximation,

$$(5.8) \quad \frac{dE_2}{dt} = \mathbf{J}(\tilde{y}, t)E_2 - Qf(\tilde{y}, t), \quad E_2(t_0) = -Qy_0 - \delta y_0.$$

For a uniformly selected random vector $u \in S_{n-1}$ and with λ the solution of (4.3), we have

$$(5.9) \quad \begin{aligned} u^T E_2(t_f) &= - \int_{t_0}^{t_f} \lambda^T(\tau) Qf(\tilde{y}(\tau), \tau) d\tau - \lambda^T(t_0) (Qy_0 + \delta y_0) \\ &= u^T e(t_f) - \lambda^T(t_0) \delta y_0, \end{aligned}$$

where $e(t_f)$ is the approximation error for the original system, defined by (4.1). Straightforward calculations yield

$$(5.10) \quad \|E_2(t_f)\| \leq \|e(t_f)\| + \kappa_2 \cdot \|\delta y_0\|,$$

where

$$\kappa_2 = \frac{W_q}{W_n} \sqrt{\sum_{j=1}^q \|\lambda(t_0)\|_2^2}.$$

We first note that the new condition number κ_2 has the exact same form as κ_1 obtained in section 5.1.1, the only difference being in the final conditions used for the adjoint variables λ_j . Second, the SCE bound estimate (5.10) is more accurate than the SCE bound estimate for the norm of $E_1(t_f)$ (which is based on the additional approximation $E_1 \approx e + \Delta_\perp$, ignoring Δ_S and using $y \approx \tilde{y}$ in the adjoint system). Furthermore, as seen from (5.9), an SCE estimate for $\|E_2(t_f)\|$ can be computed without need for Y or \tilde{Y} , unlike for $\|E_1(t_f)\|$.

5.2. Perturbations in Model Parameters. Now let Y be the solution of the ODE system

$$(5.11) \quad \frac{dY}{dt} = f(Y, t, p + \delta p), \quad Y(t_0) = y_0,$$

representing a perturbation in some model parameters affecting the right-hand side of (2.1). As in section 5.1, let \tilde{Y} be the solution of a POD-based reduced-order model obtained from (5.11) using the same POD projection matrix as for the model reduction of the unperturbed system. Then \tilde{Y} satisfies

$$\frac{d\tilde{Y}}{dt} = Pf(\tilde{Y}, t, p + \delta p), \quad \tilde{Y}(t_0) = Py_0.$$

5.2.1. Estimation of $E_1 = \tilde{\mathbf{Y}} - \mathbf{Y}$. Similar to section 5.1.1, we decompose the error $\Delta = E_1 - e$ into its components $\Delta_\perp \in S^\perp$ and $\Delta_S \in S$. We retain only the first-order term from the Taylor expansion of Δ_\perp around $\delta p = 0$,

$$\Delta_\perp = -Q \left. \frac{dY}{d\delta p} \right|_{\delta p=0} \delta p.$$

The sensitivity matrix $\Psi = dY/d\delta p$ satisfies

$$\frac{d\Psi}{dt} = \mathbf{J}(y, t, p)\Psi + \mathbf{K}(y, t, p), \quad \Psi(t_0) = 0,$$

where $\mathbf{K} = \partial f/\partial p$ is the Jacobian of f with respect to p . In terms of the fundamental matrix Φ of the linearization of (2.1), we have

$$\Psi(t_f) = \int_{t_0}^{t_f} \Phi(t_f)\Phi^{-1}(\tau)\mathbf{K}(y(\tau), \tau, p) d\tau,$$

and thus

$$u^T \Delta_\perp(t_f) = - \left(\int_{t_0}^{t_f} \lambda^T(\tau)\mathbf{K}(y(\tau), \tau, p) d\tau \right) \cdot \delta p,$$

where λ is the solution of (5.5) and $u \in R^n$.

The observations in section 5.1.1 remain valid: (a) using vectors u' from the S_{n-k-1} sphere embedded in S^\perp gives a more accurate SCE error norm estimate; (b) a more efficient adjoint solution can be obtained assuming $\mathbf{J}(y, t, p) \approx \mathbf{J}(\tilde{y}, t, p)$ and $\mathbf{K}(y, t, p) \approx \mathbf{K}(\tilde{y}, t, p)$.

The SCE estimate of the norm of Δ_\perp is then

$$\|\Delta_\perp(t_f)\| \approx \frac{W_q}{W_n} \sqrt{\sum_{j=1}^q \left| \int_{t_0}^{t_f} \lambda^T(\tau)\mathbf{K}(\tilde{y}(\tau), \tau, p) \delta p d\tau \right|^2},$$

bounded by $\|\Delta_\perp(t_f)\| \leq \kappa_1 \cdot \|\delta p\|$, where κ_1 is now defined as

$$\kappa_1 = \frac{W_q}{W_n} \sum_{j=1}^q \|\lambda^T \mathbf{K}\|_{L_1}^2.$$

In complete analogy with section 5.1.1, if $\mathbf{J}(y, t, p) \approx \mathbf{J}(\tilde{y}, t, p)$ and $\mathbf{K}(y, t, p) \approx \mathbf{K}(\tilde{y}, t, p)$, the component Δ_S parallel to S satisfies to a first-order approximation

$$\frac{d\Delta_S}{dt} = P\mathbf{J}(\tilde{y}, t, p)\Delta_S, \quad \Delta_S(t_0) = 0,$$

and therefore $\Delta_S(t) = 0$ for all $t \geq t_0$. As a consequence, $\Delta(t_f) \approx \Delta_\perp(t_f)$ and

$$\|E_1(t_f)\| \leq \|e(t_f)\| + \kappa_1 \cdot \|\delta p\|_\infty.$$

5.2.2. Estimation of $E_2 = \tilde{\mathbf{y}} - \mathbf{Y}$. Following a similar approach to section 5.2.1, for a uniformly selected random vector $u \in S_{n-1}$ and with $\lambda_{\tilde{y}}$ the solution of (4.3),

$$\begin{aligned} u^T E_2(t_f) &= - \int_{t_0}^{t_f} \lambda^T(\tau) \left[Qf(\tilde{y}(\tau), \tau, p) + \mathbf{K}(\tilde{y}(\tau), \tau, p) \delta p \right] d\tau \\ (5.12) \quad &\quad - \lambda^T(t_0) Q y_0 \\ &= u^T e(t_f) - \int_{t_0}^{t_f} \lambda^T(\tau) \mathbf{K}(\tilde{y}(\tau), \tau, p) \delta p d\tau, \end{aligned}$$

where $e(t_f)$ is the approximation error for the original system, defined by (4.1). As in section 5.1.2, it follows that

$$(5.13) \quad \|E_2(t_f)\| \leq \|e(t_f)\| + \kappa_2 \cdot \|\delta p\|_\infty,$$

where the condition number κ_2 is now

$$\kappa_2 = \frac{W_q}{W_n} \sqrt{\sum_{j=1}^q \|\lambda^T \mathbf{K}\|_{L_1}^2}.$$

The above SCE bound estimate for the norm of $E_2(t_f)$ is again more accurate than the one derived in section 5.2.1 for the bound on the norm of $E_1(t_f)$. Furthermore, starting from (5.12), an SCE estimate for $\|E_2(t_f)\|$ can be computed without need for Y or \tilde{Y} , unlike for $\|E_1(t_f)\|$ in section 5.2.1.

6. Examples. We consider reduced-order ODE examples that are representative of problems derived from spatial discretization of PDEs (linear advection-diffusion) or directly obtained from physical phenomena (a pollution model). Additional examples are described in [13].

For each example, two figures with numerical results are provided (Figures 4 and 5 for the first example and Figures 6 and 7 for the second one). The estimates (and bounds) were obtained using $q = 1$ (blue), $q = 2$ (green), and $q = 3$ (red), where q is the number of orthogonal vectors used by the SCE.

Figure 4 contains POD approximation errors as functions of the dimension of the subspace S . The norm of the total approximation error at the final time, $\|e(t_f)\| = \|\tilde{y}(t_f) - y(t_f)\|$, is given in plot (a), while the norm of the subspace integration error at the final time, computed in the subspace S , i.e., $\|e_S(t_f)\|$, is presented in plot (b). The solid (black) lines represent the corresponding norms computed by the forward integration of the error equations (4.2) and (4.8), respectively. The dotted (colored) lines describe SCE estimates (4.5) and (4.10), respectively, for different values of q . The dashed (colored) lines appear only in plot (b) and represent the bounds of (4.11) for different values of q .

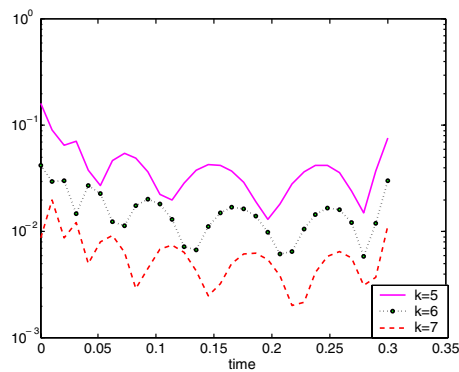
The first four plots in Figure 5 contain estimates of errors induced by a perturbation δy_0 in the initial conditions. Plot (a) presents the norm of the total approximation error of the perturbed system at the final time, $\|E_1(t_f)\| = \|\tilde{Y}(t_f) - Y(t_f)\|$, as a function of the subspace dimension k . Plot (b) contains the norm of the cumulative error of the perturbed system at the final time, $\|E_2(t_f)\| = \|\tilde{y}(t_f) - Y(t_f)\|$, as a function of the subspace dimension k . Plots (c) and (d) present the error bounds for $\|E_1(t_f)\|$ and $\|E_2(t_f)\|$, respectively, as predicted by the condition numbers κ_1 and κ_2 over a range of perturbations δy_0 , for a given value of k . The solid (black) line represents the norm computed by the forward integration of the error equations (5.3) and (5.8), respectively. For different values of q , the dashed (colored) lines represent SCE estimates of the upper bound of (5.7) in plots (a) and (b), and of (5.10) in plots (c) and (d). For different values of q , the dotted (colored) lines represent SCE estimates for $\|E_1(t_f)\|$ in plot (a) and for $\|E_2(t_f)\|$ in plot (b).

The last four plots in Figure 5 contain estimates of errors induced by a perturbation δp in the model parameters. The corresponding plots (e), (f), (g), and (h) are in a format which is analogous to the one above.

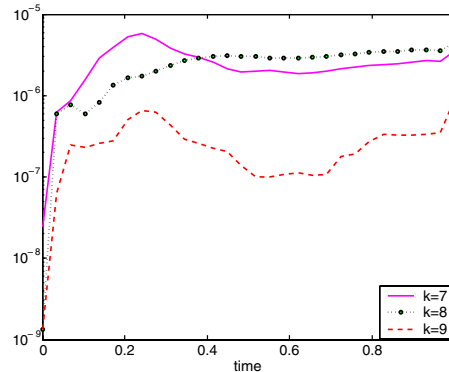
The (blue) line made of circles represents the norm of the true (nonlinear) error, $e(t) = \tilde{y}(t) - y(t)$, where \tilde{y} is the solution of (2.4) and y is the solution of (2.1).

Table 1 The sum of ignored eigenvalues Λ_k and their relative size Λ .

k	Example 1: Advection-diffusion		Example 2: Pollution model	
	Λ_k	Λ	Λ_k	Λ
5	1.803561e-01	5.890413e-06	6.341930e-13	2.652438e-12
6	2.831234e-02	9.246781e-07	6.971282e-14	2.915657e-13
7	4.193422e-03	1.369567e-07	1.139176e-15	4.764470e-15
8	5.662276e-04	1.849294e-08	1.175776e-16	4.917547e-16
9	6.944298e-05	2.268001e-09	4.938977e-17	2.065669e-16
10	7.716002e-06	2.520038e-10	9.158667e-18	3.830506e-17



(a) 1-D advection-diffusion example



(b) Pollution example

Fig. 3 The norm of the total model-reduction error $\|e\| = \|y - \tilde{y}\|$ vs. time, with y the solution of the full model and \tilde{y} the solution of the reduced model.

Dimension of the POD Subspace. Let $\Lambda_k = \sum_{i=k+1}^n \lambda_i$ be the sum of the eigenvalues ignored in the construction of the POD-reduced model and let $\Lambda = \Lambda_k / \sum_{i=1}^n \lambda_i$ be its relative size compared to the sum of all eigenvalues. The POD subspace dimension k is selected such that the relative error is very close to one, yet k is sufficiently small. A relative error near zero means that a high percentage of the energy for the full model was captured by the reduced-order model. The values of Λ_k and Λ , for the numerical examples considered in this paper, are presented in Table 1.

To assess how well the full model is approximated by the POD-based reduced model, we present in Figure 3 the behavior of the norm of the total error over the given time interval for both examples considered in the paper. The dimension of the POD subspace is denoted by k and has values (5, 6, 7) for the one-dimensional (1-D) advection-diffusion example and (7, 8, 9) for the pollution example.

Number of Orthogonal Vectors for the SCE Estimate. We considered one, two, and three SCE vectors for our numerical examples. As expected, having just one SCE vector yielded the worst estimate in most of the cases. Nevertheless, even that estimate was, in many cases, good enough to warrant its inclusion in our results.

6.1. Linear Advection-Diffusion Model.

We consider the 1-D problem

$$u_t = p_1 u_{xx} + p_2 u_x$$

with boundary conditions $u(0, t) = u(2, t) = 0$

and initial conditions $u(x, 0) = u_0(x) = x(2 - x)e^{2x}$.

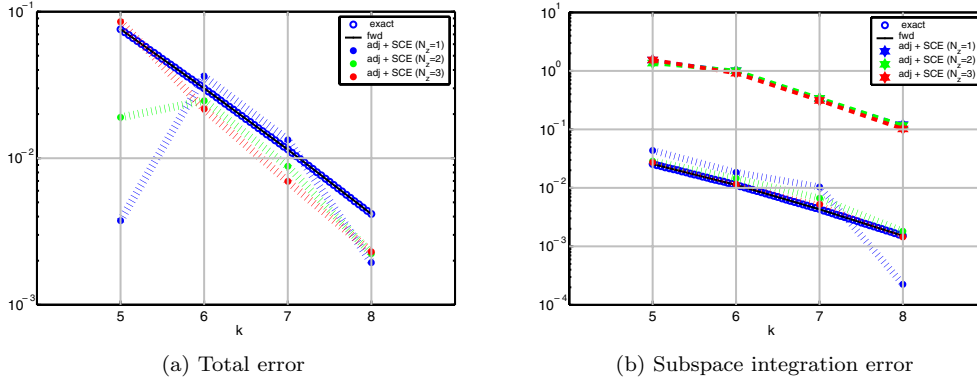


Fig. 4 1-D advection-diffusion example. Model-reduction error.

The PDE is discretized on a uniform grid of size $n + 2$ with central differencing. With $y_i(t) = u(x_i, t)$ and eliminating boundary values, we obtain the following size n ODE system:

$$\frac{dy_i}{dt} = p_1 \frac{y_{i+1} - 2y_i + y_{i-1}}{\Delta x^2} + p_2 \frac{y_{i+1} - y_{i-1}}{2\Delta x}, \quad y_i(0) = u_0(x_i).$$

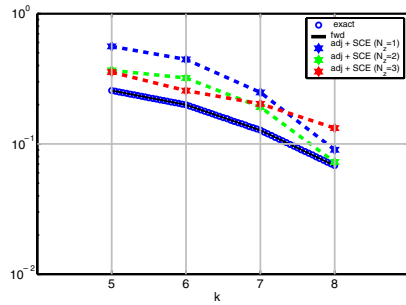
The problem parameters were $p_1 = 0.5$, $p_2 = 1.0$, and $N = 100$. Results for this problem are shown in Figures 4 and 5. The POD projection matrices were based on $m = 100$ data points equally spaced in the interval $[t_0, t_f] = [0.0, 0.3]$. The estimate of the total error is consistently close to the exact value, with the estimates corresponding to $q = 2, 3$ almost identical to the subspace integration error. The bounds are within an order of magnitude for both initial conditions and right-hand side perturbations. The right-hand side perturbation increases the distance between the bounds and the forward error. That was expected, since the right-hand side perturbation changes the advection coefficient p_2 , which is dominant for the time window considered.

6.2. Pollution Model. Next we consider the chemical reactions from an air pollution model described in [34]. This is a highly nonlinear stiff ODE system consisting of 25 reactions and 20 species. The problem is of the form

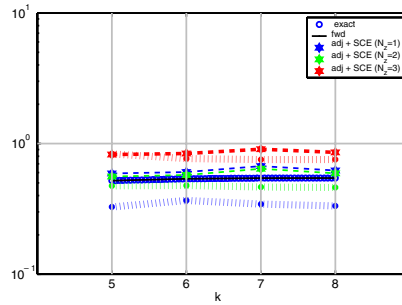
$$\frac{dy}{dt} = f(y), \quad y(0) = y_0, \quad y \in R^{20},$$

where the function $f(y)$ is defined by

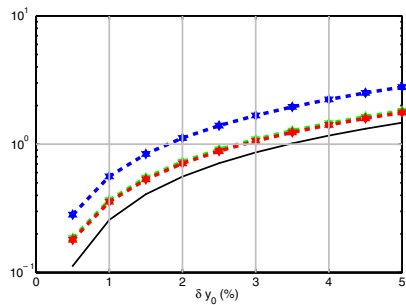
$$\begin{aligned} f_1 &= -\sum_{j \in \{1,10,14,23,24\}} r_j + \sum_{j \in \{2,3,9,11,12,22,25\}} r_j, & f_{12} &= r_9, \\ f_2 &= -r_2 - r_3 - r_9 - r_{12} + r_1 + r_{21}, & f_{14} &= -r_{13} + r_{12}, \\ f_3 &= -r_{15} + r_1 + r_{17} + r_{19} + r_{22}, & f_{18} &= r_{20}, \\ f_4 &= -r_2 - r_{16} - r_{17} - r_{23} + r_{15}, & f_{13} &= -r_{11} + r_{10}, \\ f_5 &= -r_3 + r_4 + r_4 + r_6 + r_7 + r_{13} + r_{20}, & f_{17} &= -r_{20}, \\ f_6 &= -r_6 - r_8 - r_{14} - r_{20} + r_3 + 2r_{18}, & f_{15} &= r_{14}, \\ f_7 &= -r_4 - r_5 - r_6 + r_{13}, & f_{16} &= -r_{18} - r_{19} + r_{16}, \\ f_8 &= r_4 + r_5 + r_6 + r_7, & f_{10} &= -r_{12} + r_7 + r_9, \\ f_{11} &= -r_9 - r_{10} + r_8 + r_{11}, & f_9 &= -r_7 - r_8, \\ f_{19} &= -r_{21} - r_{22} + r_{22} - r_{24} + r_{25}, & f_{20} &= -r_{25} + r_{24}, \end{aligned}$$



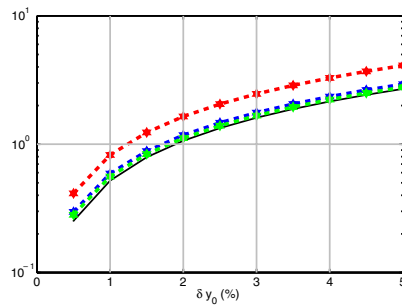
(a) E_1 for perturbations in initial conditions vs. k ($\delta y_0 = 1.0\%$)



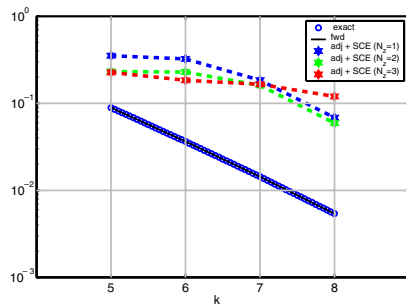
(b) E_2 for perturbations in initial conditions vs. k ($\delta y_0 = 1.0\%$)



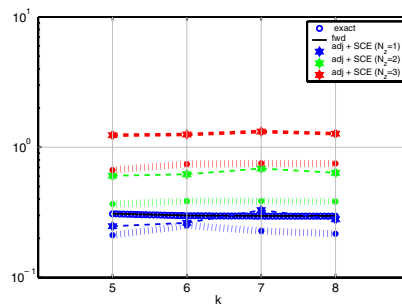
(c) E_1 vs. the perturbation in initial conditions ($k = 5$)



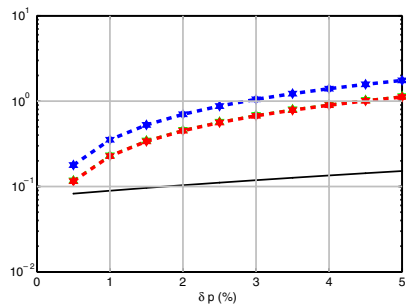
(d) E_2 vs. the perturbation in initial conditions ($k = 5$)



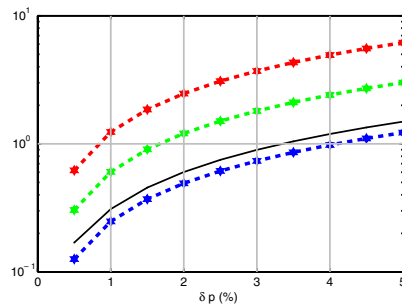
(e) E_1 for perturbations in model parameters vs. k ($\delta p = 1.0\%$)



(f) E_2 for perturbations in model parameters vs. k ($\delta p = 1.0\%$)



(g) E_1 vs. the perturbation in model parameters ($k = 5$)



(h) E_2 vs. the perturbation in model parameters ($k = 5$)

Fig. 5 1-D advection-diffusion example. Regions of validity.

Table 2 Auxiliary variables (r_j) and model parameters (k_j) for the pollution model.

$r_1 = k_1 y_1$	$r_7 = k_7 y_9$	$r_{13} = k_{13} y_{14}$	$r_{19} = k_{19} y_{16}$
$r_2 = k_2 y_2 y_4$	$r_8 = k_8 y_9 y_6$	$r_{14} = k_{14} y_{11} y_6$	$r_{20} = k_{20} y_{17} y_6$
$r_3 = k_3 y_5 y_2$	$r_9 = k_9 y_{11} y_2$	$r_{15} = k_{15} y_3$	$r_{21} = k_{21} y_{19}$
$r_4 = k_4 y_7$	$r_{10} = k_{10} y_{11} y_1$	$r_{16} = k_{16} y_4$	$r_{22} = k_{22} y_{19}$
$r_5 = k_5 y_7$	$r_{11} = k_{11} y_{13}$	$r_{17} = k_{17} y_4$	$r_{23} = k_{23} y_{19} y_4$
$r_6 = k_6 y_7 y_6$	$r_{12} = k_{12} y_{10} y_2$	$r_{18} = k_{18} y_{16}$	$r_{24} = k_{24} y_{19} y_1$
			$r_{25} = k_{25} y_{20}$
$k_1 = 0.350 \cdot 10^0$	$k_7 = .130 \cdot 10^{-3}$	$k_{13} = .188 \cdot 10^1$	$k_{19} = .444 \cdot 10^{12}$
$k_2 = 0.266 \cdot 10^2$	$k_8 = .240 \cdot 10^5$	$k_{14} = .163 \cdot 10^5$	$k_{20} = .124 \cdot 10^4$
$k_3 = .123 \cdot 10^5$	$k_9 = .165 \cdot 10^5$	$k_{15} = .480 \cdot 10^7$	$k_{21} = .210 \cdot 10^1$
$k_4 = .860 \cdot 10^{-3}$	$k_{10} = .900 \cdot 10^4$	$k_{16} = .350 \cdot 10^{-3}$	$k_{22} = .578 \cdot 10^1$
$k_5 = .820 \cdot 10^{-3}$	$k_{11} = .220 \cdot 10^{-1}$	$k_{17} = .175 \cdot 10^{-1}$	$k_{23} = .474 \cdot 10^{-1}$
$k_6 = .150 \cdot 10^5$	$k_{12} = .120 \cdot 10^5$	$k_{18} = .100 \cdot 10^9$	$k_{24} = .178 \cdot 10^4$
			$k_{25} = .312 \cdot 10^1$

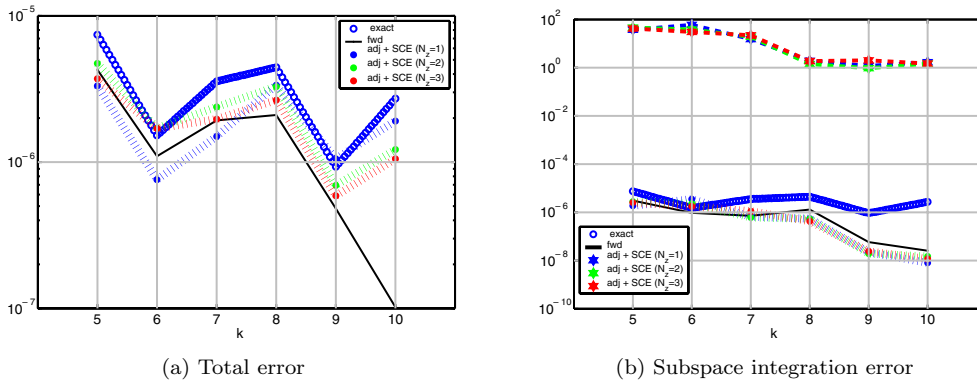


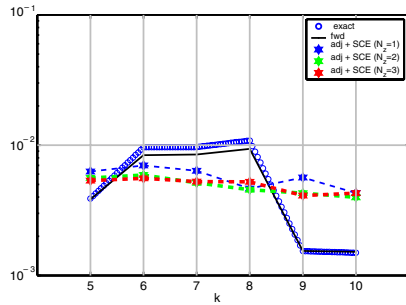
Fig. 6 Pollution example. Model-reduction error.

and $y_0 = [0, 0.2, 0, 0.04, 0, 0, 0.1, 0.3, 0.01, 0.0, 0, 0, 0, 0, 0.007, 0, 0, 0]^T$. The auxiliary variables r_j and the model parameters k_j are given in Table 2.

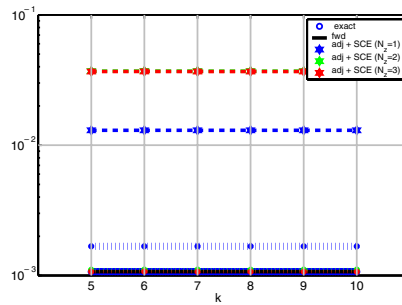
Numerical results depicting the approximation errors and the regions of validity at $t_f = 1.0$ are presented in Figures 6 and 7, respectively. The POD projection matrix was based on $m = 1000$ data points equally spaced in the interval $[t_0, t_f] = [0.0, 1.0]$.

For $k = 5, 6, 7$ the total error and the subspace integration error are very well approximated by estimates corresponding to $q = 2$ or 3. For $k = 8, 9, 10$ the estimates are not as good, although they remain within an order of magnitude. We believe that this behavior is related to the fact that the POD error (either absolute or relative) is very small. We note that the problem was solved using relative tolerances of 10^{-4} and absolute tolerance of 10^{-7} . Thus one can expect a less uniform behavior if the results are in the neighborhood of 10^{-7} .

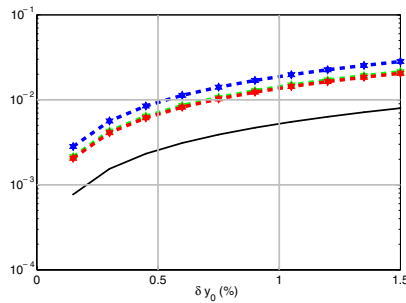
Finally, we note that due to the fact that the problem parameters k_j have orders of magnitude ranging from 10^{-3} to 10^{12} , we have limited the right-hand side perturbation only to perturbations in k_4, k_5 , and k_7 .



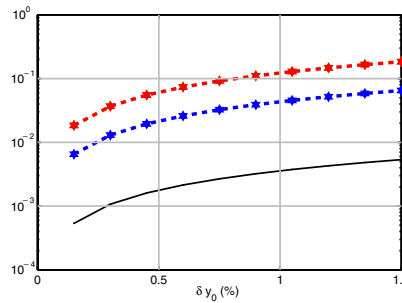
(a) E_1 for perturbations in initial conditions vs. k ($\delta y_0 = 0.3\%$)



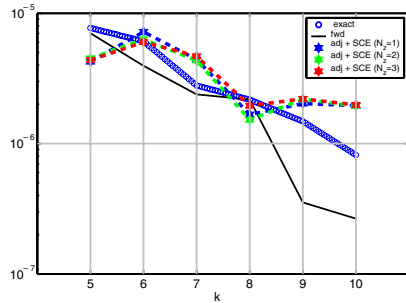
(b) E_2 for perturbations in initial conditions vs. k ($\delta y_0 = 0.3\%$)



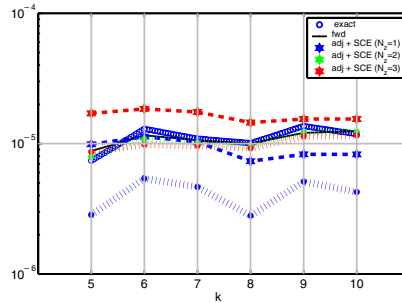
(c) E_1 vs. the perturbation in initial conditions ($k = 5$)



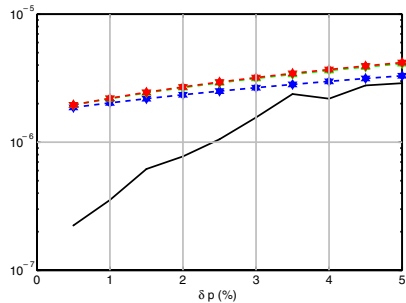
(d) E_2 vs. the perturbation in initial conditions ($k = 5$)



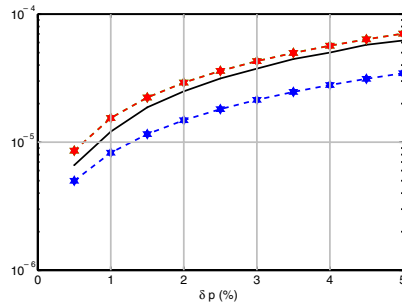
(e) E_1 for perturbations in model parameters vs. k ($\delta p = 1.0\%$)



(f) E_2 for perturbations in model parameters vs. k ($\delta p = 1.0\%$)



(g) E_1 vs. the perturbation in model parameters ($k = 5$)



(h) E_2 vs. the perturbation in model parameters ($k = 5$)

Fig. 7 Pollution example. Regions of validity.

6.3. More Examples. In [13] we include more test problems derived from spatial discretization of PDEs (Burgers' PDE or the Brusselator PDE) or directly obtained from physical phenomena (HIRES High Irradiance Response). The results obtained for those examples confirm our approach, in the sense that the SCE estimates offer a good approximation for the errors of the POD-reduced models. For more details, the reader may consult [13], which is available online.

7. Conclusions and Future Work. We have presented effective methods for estimating approximation errors due to the use of POD-based reduced-order models and for evaluating regions of validity of such reduced models. The bounds defining these regions of validity are a priori, in the sense that they do not rely on the solution of the perturbed system. The proposed approach, based on SCE norm estimates combined with the adjoint method, allows the definition and construction of so-called error condition numbers which can be used to assess the size of errors induced by perturbations (in initial conditions or in the model itself) without having to solve the perturbed system. The effectiveness of the proposed methods was demonstrated on several test problems.

We are currently investigating the applicability of this technique to the estimation of errors from other types of reduced-order models, as well as considering more complex models than those presented both in this paper and in [13]. Thus we will consider models which exhibit more interesting (e.g., oscillatory or chaotic) behavior in their POD-reduced model. For example, we think that our method to efficiently compute the error corresponding to different perturbations may be useful in conjunction with reduced models in oceanography or atmospheric sciences (recent advances [21] present POD-based reduced models that can approximate well even the bifurcation behavior of the flow).

Note Added to SIGEST Paper. Recently [30] we have extended this work to estimation of the validity of general nonlinear ROMs of dynamical systems described by ODEs and differential algebraic equations (DAEs). The proposed technique is applicable as long as adjoint models can be defined for both the full and reduced systems. The resulting estimates, based on a combination of adjoint sensitivity analysis and SCE norm estimates, quantify how well a given ROM captures the changes in the output functional of the full system that result from perturbations in the problem parameters. We introduce two types of similarity indices to measure the extent to which the ROM preserves the value of maximum perturbation-induced error (and/or the direction of the perturbations that induce it). The direction in parameter space of maximum error growth in the output functional is efficiently computed within the framework of singular vector analysis, using the SCE estimate for the error norm.

The numerical examples presented in [30] show that the similarity index concept is very effective for detecting situations where the ROM fails to capture the behavior of the full model when the parameters are slightly perturbed. They also indicate that it is quite possible, particularly when the reduced model is constructed via automatic procedures (e.g., POD), to generate reduced models that agree well with the original data but are not robust to even small perturbations in the system parameters.

REFERENCES

- [1] U. ACHATZ AND G. BRANSTATOR, *A two-layer model with empirical linear corrections and reduced order for studies of internal climate variability*, *J. Atmospheric Sci.*, 56 (1999), pp. 3140–3160.

- [2] A.C. ANTOUNAS AND D.C. SORENSSEN, *Approximation of Large-Scale Dynamical Systems: An Overview*, Tech. report TR0101, Rice University, Houston, TX, 2001.
- [3] E. BALSACANTO, A.A. ALONSO, AND J.R. BANGA, *A novel, efficient and reliable method for thermal process design and optimization*, J. Food Engrg., 52 (2002), pp. 227–247.
- [4] Y. CAO AND L. PETZOLD, *A posteriori error estimation and global error control for ordinary differential equations by the adjoint method*, SIAM J. Sci. Comput., 26 (2004), pp. 359–374.
- [5] E. CARABALLO, M. SAMINY, J. SCOTT, S. NARAYAN, AND J. DEBONIS, *Application of proper orthogonal decomposition to a supersonic axisymmetric jet*, AIAA J., 41 (2003), pp. 866–877.
- [6] P.G.A. CIZMAS AND A. PALACIOS, *Proper orthogonal decomposition of turbine rotor-stator interaction*, J. Propul. Power, 19 (2003), pp. 268–281.
- [7] D.T. CROMMELIN AND A.J. MAJDA, *Strategies for model reduction: Comparing different optimal bases*, J. Atmospheric Sci., 61 (2004), pp. 2206–2217.
- [8] F. D’ANDREA AND R. VAUTARD, *Extratropical low-frequency variability as a low-dimensional problem I: A simplified model*, Q. J. R. Meteorol. Soc., 127 (2001), pp. 1357–1375.
- [9] K. FUKUNAGA, *Introduction to Statistical Pattern Recognition*, Academic Press, San Diego, CA, 1990.
- [10] G.H. GOLUB AND C.F. VAN LOAN, *Matrix Computations*, The Johns Hopkins University Press, Baltimore, MD, 1996.
- [11] T. GUDMUNDSSON, C.S. KENNEY, AND A.J. LAUB, *Small-sample statistical estimates for matrix norms*, SIAM J. Matrix Anal. Appl., 16 (1995), pp. 776–792.
- [12] P. HOLMES, J.L. LUMLEY, AND G. BERKOOZ, *Turbulence, Coherent Structures, Dynamical Systems and Symmetry*, Cambridge University Press, Cambridge, UK, 1998.
- [13] C. HOMESCU, L.R. PETZOLD, AND R. SERBAN, *Error Estimation for Reduced Order Models of Dynamical Systems*, Tech. report UCRL-TR-201494, Lawrence Livermore National Laboratory, Livermore, CA, 2003.
- [14] I.T. JOLLIFFE, *Principal Component Analysis*, Springer-Verlag, New York, 2002.
- [15] C.S. KENNEY AND A.J. LAUB, *Small-sample statistical condition estimates for general matrix functions*, SIAM J. Sci. Comput., 15 (1994), pp. 36–61.
- [16] H. KIKUCHI, Y. TAMURA, H. UEDA, AND K. HIBI, *Dynamic wind pressures acting on a tall building model—proper orthogonal decomposition*, J. Wind Eng. Ind. Aerod., 71 (1997), pp. 631–646.
- [17] M.E. KOWALSKI AND H.M. JIN, *Model-order reduction of nonlinear models of electromagnetic phased-array hyperthermia*, IEEE T. Bio-Med. Eng., 50 (2003), pp. 1243–1254.
- [18] K. KUNISCH AND S. VOLKWEIN, *Control of the Burgers equation by a reduced-order approach using proper orthogonal decomposition*, J. Optim. Theory Appl., 102 (1999), pp. 345–371.
- [19] K. KUNISCH AND S. VOLKWEIN, *Galerkin proper orthogonal decomposition methods for a general equation in fluid dynamics*, SIAM J. Numer. Anal., 40 (2002), pp. 492–515.
- [20] P.A. LEGRESLEY AND J.J. ALONSO, *Dynamic Domain Decomposition and Error Correction for Reduced Order Models*, AIAA Paper 2003-0250, 41st AIAA Aerospace Sciences Meeting & Exhibit, Reno, NV, 2003.
- [21] C. LOPEZ AND E. GARCIA-HERNÁNDEZ, *Low-dimensional dynamical system model for observed coherent structures in ocean satellite data*, Phys. A, 328 (2003), pp. 233–250.
- [22] D.J. LUCIA, P.I. KING, M.E. OXLEY, AND P.S. BERAN, *Reduced Order Modeling for a One-Dimensional Nozzle Flow with Moving Shocks*, AIAA Paper 01-2602, AIAA 15th Computational Fluid Dynamics Conference, Anaheim, CA, 2001.
- [23] X. MA AND G.E. KARNIADAKIS, *A low-dimensional model for simulating three-dimensional cylinder flow*, J. Fluid Mech., 458 (2002), pp. 181–190.
- [24] A.J. MAJDA, I. TIMOFEYEV, AND E. VANDEN-ELJNDEN, *Systematic strategies for stochastic mode reduction in climate*, J. Atmospheric Sci., 60 (2003), pp. 1705–1722.
- [25] M. MEYER AND H.G. MATTHIES, *Efficient model reduction in non-linear dynamics using the Karhunen–Loeve expansion and dual-weighted-residual methods*, Comput. Mech., 31 (2003), pp. 179–191.
- [26] M. RATHINAM AND L.R. PETZOLD, *A new look at proper orthogonal decomposition*, SIAM J. Numer. Anal., 41 (2003), pp. 1893–1925.
- [27] S.S. RAVINDRAN, *A reduced-order approach for optimal control of fluids using proper orthogonal decomposition*, Internat. J. Numer. Methods Fluids, 34 (2000), pp. 425–448.
- [28] J.A. RULE, R.E. RICHARD, AND R.L. CLARK, *Design of an aeroelastic delta wing model for active flutter control*, J. Guid. Control Dynam., 24 (2001), pp. 918–924.
- [29] F.M. SELTEN, *Baroclinic empirical orthogonal functions as basis functions in an atmospheric model*, J. Atmospheric Sci., 54 (1997), pp. 2100–2114.

- [30] R. SERBAN, L.R. PETZOLD, AND C. HOMESCU, *The effect of problem perturbations on nonlinear dynamical systems and their reduced order models*, SIAM J. Sci. Comput., submitted (2006).
- [31] B. SHAPIRO, *Creating compact models of complex electronic systems: An overview and suggested use of existing model reduction and experimental system identification tools*, IEEE T. Comp. Pack. T., 26 (2003), pp. 165–172.
- [32] Y. SHIN AND T. SAKURAI, *Power distribution analysis of VLSI interconnects using model order reduction*, IEEE T. Comput. Aid. D., 21 (2002), pp. 739–745.
- [33] S. UTKU, J.L.M. CLEMENTE, AND M. SALAMA, *Errors in reduction methods*, Comput. & Structures, 21 (1985), pp. 1153–1157.
- [34] J.G. VERWER, *Gauss–Seidel iteration for stiff ODEs from chemical kinetics*, SIAM J. Sci. Comput., 15 (1994), pp. 1243–1250.